Available online at www.ijournalse.org

Emerging Science Journal

(ISSN: 2610-9182)

Vol. 10, No. 2, April, 2026

Castor-Based Ester Oil Production Using $SnCl_2$/HZSM-5 Catalyst for Sustainable Transformer

Istiqomah [1], Widayat Widayat [2, 3], John Philia [3], Sriyono [1], Kevin Gausultan Hadith Mangunkusumo [1], Aji Suryo Alam [1], Hadiyanto [2, 4*]

[1] *Transmission and Distribution Department, PLN Research Institute, Jakarta 12760, Indonesia.*

[2] *Department of Chemical Engineering, Faculty of Engineering, Diponegoro University, Semarang 50275, Indonesia.*

[3] *Advanced Materials Laboratory, Diponegoro University, Semarang 50275, Indonesia.*

[4] *Center of Biomass and Renewable Energy (CBIORE), Diponegoro University, Semarang 50275, Indonesia.*

Abstract

Mineral oil remains the most common insulating fluid in power transformers; nevertheless, its non-biodegradable nature and carbon-based emissions have prompted the quest for environmentally safer alternatives. Castor oil, a sustainable and non-edible derivative, provides a promising source for high-performance ester-based insulating lubricants. This study investigates the synthesis and process optimization of castor-based polyol esters via esterification with trimethylolpropane using a heterogeneous $SnCl_2$/HZSM-5 catalyst. The alcohol-to-oil molar ratio, temperature, and catalyst loading were among the critical reaction parameters that were modeled and optimized using response surface methods with a central composite design. Under optimized conditions of 130°C and 2.207 wt% catalyst, an ester yield of 81.77% was obtained. The resulting ester oil demonstrated advantageous characteristics, such as acceptable color and dielectric performance, while viscosity and acidity were improved by a two-step process to comply with the IEC 62975:2021 standards for distribution transformer insulating oils. The statistical study validated the model's reliability, with ANOVA indicating a substantial quadratic regression ($R^2 = 0.952$). The key novelty of this work lies in demonstrating the potential of $SnCl_2$/HZSM-5 to catalyze the synthesis of castor-derived polyol esters with tailored physicochemical properties, supporting their future scalability and use as sustainable insulating oils.

Keywords:

Castor;
Trimethylolpropane;
Tin (II) Dichloride;
Optimization;
Eco-Friendly.

Article History:

Received:	15	June	2025
Revised:	27	January	2026
Accepted:	03	March	2026
Published:	01	April	2026

1- Introduction

Transformer insulation oils have evolved significantly since paraffinic mineral oils were first used in the 1890s and naphthenic oils in 1925. In the 1930s, polychlorinated biphenyls (PCBs) were introduced to improve thermal and dielectric qualities; however, their environmental and health risks led to their prohibition in 1978 [1]. Silicone oils for transformers appeared in the early 1970s [2]. Mineral oils are non-biodegradable and produce carbon-based gases, making them environmentally harmful despite their good thermal and dielectric qualities [3]. These gases react with atmospheric air to form acidic compounds, contributing to acid rain formation and degradation of air quality [4]. Eco-friendly insulating materials, such as natural ester oils, have been developed to address these environmental concerns. Since the early 1990s, natural esters have gained popularity due to their lower cost and greater sustainability than synthetic oil. The Coordinating European Council (CEC-L-33) found that natural ester oils biodegrade 97%–99% due to the absence of halogens, polycyclic aromatic hydrocarbons, and volatile organic chemicals. Therefore, natural esters may enhance the environmental sustainability of transformer insulation systems.

* **CONTACT**: hadiyanto@live.undip.ac.id

DOI: https://doi.org/10.28991/ESJ-2026-010-02-06

As a renewable insulating oil, vegetable oil-based insulating oils have garnered considerable attention due to their environmental sustainability, high biodegradability, and excellent dielectric and thermal properties. Various studies have pointed to the use of vegetable oils, notably soy, sunflower, and rapeseed oils, as mineral oil-based transformer insulation fluid substitutes because of their favorable environmental and functional properties [5, 6]. On the other hand, these oils also have inherent problems, including oxidative stability and viscosity, which require further modification [7, 8]. Preliminary investigation studies on modifying vegetable oil-based insulating oils to improve their dielectric strength, thermal stability, and oxidative resistance for use in power transformers have already been published [9]. However, edible vegetable oils (such as soy, sunflower, and rapeseed oils) compete with food resources, addressing the growing concerns over food security and ethical sourcing [10, 11].

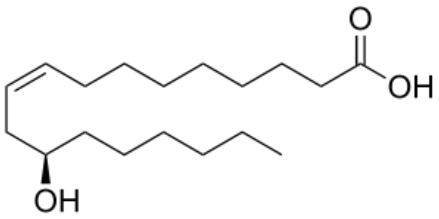

Figure 1. Molecular structure of castor oil

Castor oil (Figure 1) is a non-edible vegetable oil that exhibits biodegradability and has the potential to mitigate environmental risks [12]. Using biodegradable oils, such as castor oil, can reduce the environmental impact of electrical insulation systems, particularly in high-voltage applications [13]. The primary component of castor oil, ricinoleic acid, has a molecular structure conducive to forming esters, amides, and polymers, which are essential for insulation applications [14, 15]. Due to the presence of hydroxyl groups in ricinoleic acid, the oil can form natural polyols that enhance the chemical stability of the oil and serve as reactive sites for further modifications [16]. Castor oil can be modified through esterification and transesterification to produce fatty acid methyl ester (FAME), as an insulating ester oil (Figure 2).

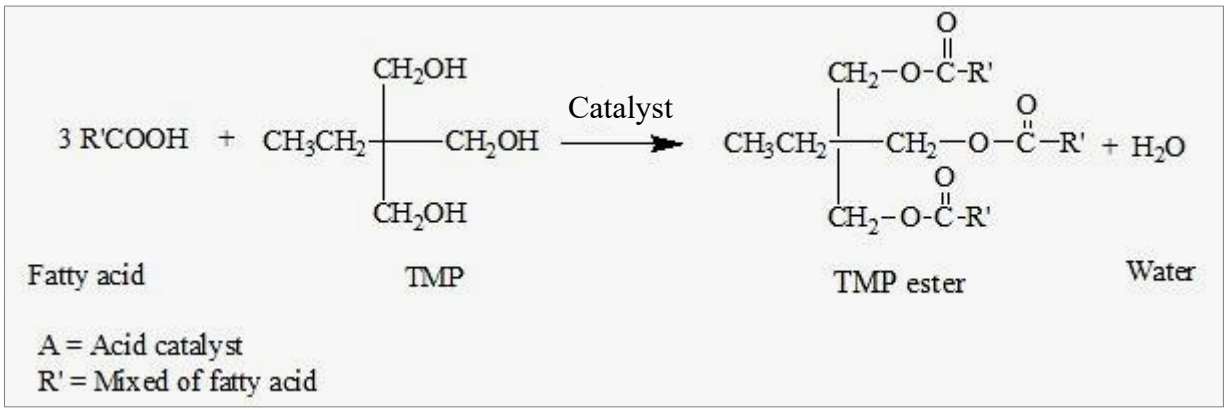

Figure 2. Esterification reaction of castor oil and TMP

Tin(II) chloride ($SnCl_2$) serves as an efficient precursor for heterogeneous Lewis acid catalysts in ester oil production, attributed to its robust electron-accepting characteristics, carbonyl-activating capacity, and compatibility with polyol–fatty acid systems. Upon deposition on solid substrates like TiO_2, $SnCl_2$ produces finely dispersed SnO_x or Sn–O surface species that generate medium-strength Lewis acid sites suitable for esterification [17]. Its characteristics and high catalytic activity enable it to promote reactions under milder conditions compared to conventional catalysts [18]. The investigation of SnO/TiO_2 reveals that catalysts prepared from $SnCl_2$ attain conversions of up to 99.6% for TMP and n-octanoic acid, demonstrating remarkable recyclability and validating the catalytic efficacy of well-dispersed Sn species. The characterization results indicate that the addition of Sn markedly enhances Lewis acidity compared to the unmodified support, hence directly improving esterification activity [19]. Moreover, findings on Lewis acid catalysis in biodiesel systems indicate that Sn^{2+} centers exhibit greater acidity and stronger carbonyl binding than Zn-based Lewis acids, thereby elucidating the superior catalytic efficacy of $SnCl_2$-based systems in esterification and transesterification reactions [20].

$SnCl_2$ has been demonstrated to efficiently catalyze the formation of methyl esters from vegetable oils, even in the presence of free fatty acids (FFAs) and water, highlighting its robustness and versatility [17]. Unlike traditional acid catalysts commonly used in ester oil production, $SnCl_2$ is less corrosive, reducing industrial equipment maintenance costs. This property also reduces the environmental impact associated with the disposal of corrosive waste products.

Other Lewis acids, including $AlCl_3$ and $FeCl_3$, frequently undergo significant hydrolysis upon exposure to trace amounts of water, resulting in the formation of metal hydroxides and the release of HCl. This corrosive by-product accelerates ester cleavage, promotes side reactions, and damages equipment [22-24]. Water is generated in situ during the esterification of free fatty acids or ricinoleic acid constituents with TMP, indicating that, even when the system initially approaches anhydrous conditions, the reaction intrinsically produces minor amounts of water that facilitate subsequent hydrolysis [24]. $SnCl_2$-derived heterogeneous catalysts avoid these issues due to the immobilization of their Lewis acid sites on the support, which exhibits resistance to chloride hydrolysis. $SnCl_2$ eliminates the need for post-reaction neutralization, simplifying the biodiesel production process and reducing the generation of waste salts, a common byproduct when using mineral acids [25].

HZSM-5 serves as a proficient support for $SnCl_2$-based heterogeneous catalysts in the esterification process involving castor oil and trimethylolpropane (TMP). Its unique microporous–mesoporous structure, elevated surface area, and inherent acidity markedly improve the dispersion, stability, and catalytic performance of Sn species [26-28]. Investigations on mesoporous $SnCl_2$@HZSM-5 systems indicate that the immobilization of $SnCl_2$ on HZSM-5 produces a composite catalyst characterized by enhanced total acidity and a well-balanced weak-to-moderate acid strength. This phenomenon arises from the formation of Si–O–Sn linkages and the presence of both Lewis and Brønsted acid sites. The collective attributes enhance polyol conversion while mitigating side reactions, as evidenced by the elevated conversion and selectivity attained in the esterification of pentaerythritol [28]. The hierarchical porosity of HZSM-5 holds significant importance, as the esterification process of castor oil and TMP entails the involvement of bulky, viscous molecules that frequently encounter diffusion constraints within solid catalysts. The presence of mesopores enhances the transport efficiency of long-chain ricinoleate and polyol molecules, whereas the microporous MFI channels facilitate shape-selective access to Sn sites. This amalgamation diminishes diffusion resistance and improves catalytic accessibility, resulting in elevated conversion and selectivity [29]. Furthermore, employing ZSM-5 as a solid support eliminates the limitations inherent in homogeneous Lewis acids, including issues of corrosion, difficulties in separation, and catalyst loss, by offering a thermally stable, recyclable, and structurally sound framework for the immobilisation of Sn species [30]. Consequently, $SnCl_2$/HZSM-5 integrates the potent carbonyl-activation capability of Sn^{2+} with the beneficial acidity, porosity, and stability of ZSM-5, rendering it exceptionally appropriate for the synthesis of high-purity ester oils from castor oil and TMP under heterogeneous catalytic circumstances.

Given these challenges, there remains a critical need for catalytic strategies that efficiently activate hydroxyl-rich triglycerides and multifunctional polyols while preserving advantageous transport properties under reaction conditions. Hierarchical zeolites such as HZSM-5 offer improved molecular diffusion and tunable acidity, making them attractive hosts for Lewis-acid metal species, including Sn^{2+}. Despite its potential, the use of castor oil in the synthesis of polyol ester oils remains underexplored, with insufficient research systematically linking the catalyst's properties to the physicochemical and dielectric characteristics of the final product. Therefore, this study aims to develop a heterogeneous $SnCl_2$/HZSM-5 catalyst specifically for the esterification of castor oil with TMP and to optimize reaction parameters using response surface methodology to achieve high ester yield under energy-efficient conditions. The findings are expected to provide new insights into the potential of castor-derived polyol esters as sustainable, insulating, and lubricating oils derived from non-edible feedstocks. This paper initially describes the preparation of the $SnCl_2$/HZSM-5 catalyst and its application in esterification, followed by an assessment of the physicochemical and dielectric properties of the synthesized ester oils, and concludes with the optimization results and their implications for industrial use.

2- Materials and Methods

2-1- Materials

Ester oil production used castor (*Ricinus communis*) oil from Semarang, Indonesia, and Trimethylolpropane ($C_6H_{14}O_3$, 98% purity, Lanxess). The chemicals and solvent used for catalyst preparation were Tin (II) dihydrate ($SnCl_2.2H_2O$, pro-analysis, PT. Smart Lab Indonesia), HZSM-5 (commercial HZSM-5, 100% purity, China), and ethanol (C_2H_6O, 96% purity, Hepichem). Sodium hydroxide (NaOH, pro-analysis, Merck) and methanol (CH_4O, technical grade, Hepichem) were required for %FFA analysis of castor oil. Filter paper (Whatman, Ø 110 mm, standard grade) was also used in catalyst preparation.

2-2- Methods

The research workflow in this study comprises four integrated stages, as shown in Figure 3. Initially, a heterogeneous $SnCl_2$/HZSM-5 catalyst was prepared by impregnation. Afterwards, ester oil was synthesized from castor oil and trimethylolpropane under various reaction conditions to evaluate catalytic efficiency and product formation behavior. The resulting ester oils were subsequently subjected to detailed physicochemical and electrical characterization to assess their suitability for transformer insulation applications based on IEC 62975:2021 criteria. Finally, statistical optimization employing response surface methodology (RSM) with a central composite design facilitated a quantitative assessment of the influence of temperature, catalyst dosage, and reactant molar ratio on ester yield and properties, providing predictive insights into process improvement and potential for future scale-up. Overall, this methodology offers a comprehensive assessment of catalyst effectiveness, product functionality, and the feasibility of castor-derived ester oils as eco-friendly transformer insulating fluids.

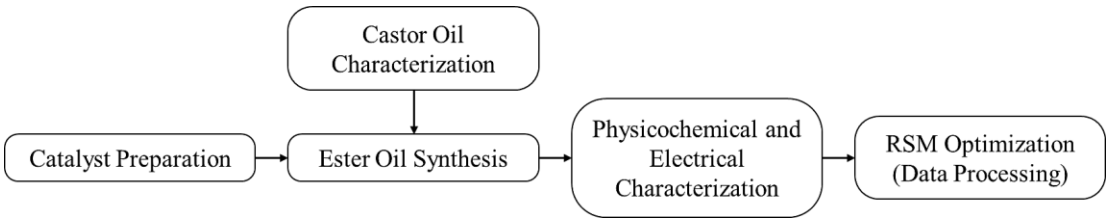

Figure 3. Flowchart of the Research Workflow

- ***Preparation and Characterization of $SnCl_2$/HZSM-5 Catalyst***

The $SnCl_2$/HZMS-5 catalyst was prepared by a wet impregnation method. Tin (II) dihydrate (0.5 grams) was dissolved in ethanol (100 ml), followed by the addition of HZSM-5 (50 grams). Then, the mixture was stirred by using a magnetic stirrer at room temperature overnight. The ethanol was removed through filtration using Whatman filter paper. $SnCl_2$/HZMS-5 was dried by using an oven at 105°C for 4 hours, and finally, the catalyst was calcined at 550°C for 5 hours in a furnace.

Scanning Electron Microscopy (SEM) with Energy Dispersive X-ray (EDX) analysis was conducted using a JEOL JSM-6510LA SEM-EDX with an accelerating voltage of 20 kV to observe the surface morphology, elemental composition, and mapping of the samples (HZSM-5 and $SnCl_2$/HZSM-5). The crystal structure and phase of the samples were examined by X-ray Diffraction (XRD) analysis, where the diffraction patterns were recorded from 10-90 o2θ using XRD-7000 with Cu K-α radiation at 30 kV and 30 mA. The surface area and pore properties of the samples were identified by physisorption analysis. The Brunauer-Emmett-Teller (BET) method was employed to measure the total area, while the average pore diameter and pore volume were calculated by the Barrett-Joyner-Halenda (BJH) method.

- ***Ester Oil Production and Characterization***

Prior to ester oil production, gas chromatography-mass spectrometry (GC-MS) analysis was performed to identify the fatty acid composition and molecular weight. Then, the %FFA content of the castor oil was observed by the acid-base titration. 5 mL of castor oil was mixed with 5 mL of methanol, and then two drops of Phenolphthalein indicator were added. The mixture was then titrated with 0.1 N NaOH until a pink color persisted in the mixture. The FFA content was calculated by using the following equation:

$$\% \text{ FFA} = \frac{\text{NaOH volume (mL)} \times \text{ NaOH normality (0,1 N)} \times \text{ fatty acid molecular weight}}{\rho \text{ castor oil} \times \text{castor oil volume} \times 1000} \times 100 \quad (1)$$

Ester oil production was conducted through the esterification and transesterification reactions of castor oil and trimethylolpropane (TMP), with a molar ratio of 3.5:1. The castor oil was poured into a 1000 mL three-neck flask and then heated to the operating temperature. After the operation temperature was reached, TMP and a specified amount of catalyst were added to the flask, and the mixture was stirred for 4 hours. The Liebig condenser was fitted into the three-necked flask and connected to a cooler (CCP5-15, DLAB, China) to maintain the cooling water at 19-20°C. After the esterification and transesterification processes, the catalyst was separated from the product by centrifugation (DMO 412, Scilogex, USA) at 3000 rpm for 10 minutes. Water, as a byproduct of the transesterification reaction, was evaporated using a vacuum oven (DZF-6020, MTI Corporation, USA) at 60°C for 2 hours. Finally, fatty acid methyl ester (FAME) or ester oil was obtained.

The physicochemical properties, including color, density, viscosity, acidity, and the PCB content of the oil ester product, were observed. The density was measured by using a pycnometer, while the viscosity was observed using Brookfield viscometer. The Fourier transform infrared (FTIR) analysis was performed to identify the functional groups of the ester oil, while the PCB and FAME content were examined through gas chromatography-mass spectrometry (GC-MS) analysis. The yield of ester oil (%FAME) was calculated using Equation 2:

$$\% \text{ Yield} = \frac{\% \text{ Area FAME based on GCMS} \times \text{biodiesel mass}}{\text{feed mass}} \times 100 \quad (2)$$

- ***Optimization of Ester Oil Production Process***

In this study, the Central Composite Design Response Surface Method is employed to optimize the yield of ester oil. The response surface method employs statistical and mathematical techniques to construct a mathematical model, identifying the optimal values of the independent variable that maximize the response variable for process development, improvement, and optimization [31-34]. This strategy is designed to optimize castor oil ester yields. The experimental design for optimizing ester oil production established the independent variables' higher (+) and lower (-) boundaries, including operating temperature and catalyst percentage. Table 1 displays the experimental design for optimizing ester oil production from castor oil-TMP.

Table 1. Experimental design of ester oil production process optimization

Run	Sample	Variable code		Variable value	
		Operating temperature (ºC)	Catalyst loading (% oil mass)	Operating temperature (ºC)	Catalyst loading (% oil mass)
1	A	0	-√2	130	0.793
2	B	0	0	130	1.5
3	C	0	√2	130	2.207
4	D	-	+	120	2
5	E	-	-	120	1
6	F	-√2	0	115.858	1.5
7	G	+	+	140	2
8	H	√2	0	144.142	1.5
9	I	0	0	130	1.5
10	J	+	-	140	1

3- Results and Discussion

3-1- $SnCl_2$/HZSM-5 Catalyst Characterization

The SEM-EDX analysis provides essential information into the morphological and compositional alterations of HZSM-5 before $SnCl_2$ impregnation. The SEM images reveal that HZSM-5 exhibits a distinct crystalline structure with a bimodal size distribution, as shown in Figure 4. This shape is crucial for maintaining elevated surface area and catalytic efficacy. Impregnation with $SnCl_2$ significantly alters surface texture, indicating the deposition of tin (Sn) species onto the zeolite framework.

The Sn and Cl incorporation into the $SnCl_2$/HZSM-5 catalyst is confirmed by elemental analysis using EDX that is shown in Table 2. The interaction of tin species with ethanol during the impregnation process is probably the reason for the significant increase in carbon content (from 12.8% to 18.36%) seen in $SnCl_2$/HZSM-5 when compared to the unmodified HZSM-5. While a slight rise in SiO_2 content (from 56.89% to 57.74%) suggests minor structural rearrangements, the appearance of SnO_2 (1.98%) and Cl (0.59%) further validates the presence of tin chloride species. Meanwhile, the reduction in Al_2O_3 content (from 29.3% to 21.27%) suggests possible changes in the framework acidity, potentially due to partial dealumination during modification. The presence of Sn on the surface signifies effective integration, potentially affecting catalytic performance via altering acid site distribution and electrical characteristics. Elemental mapping analysis further supports these findings by demonstrating a homogeneous distribution of Sn across the $SnCl_2$/HZSM-5 surface, as displayed in Figure 5. The uniform distribution of Sn is crucial for maintaining catalytic efficiency, as it prevents localized agglomeration and ensures the availability of active sites. This attribute aligns with prior research on metal-modified zeolites, where uniform metal distribution is crucial for enhancing catalytic selectivity and stability [35-37].

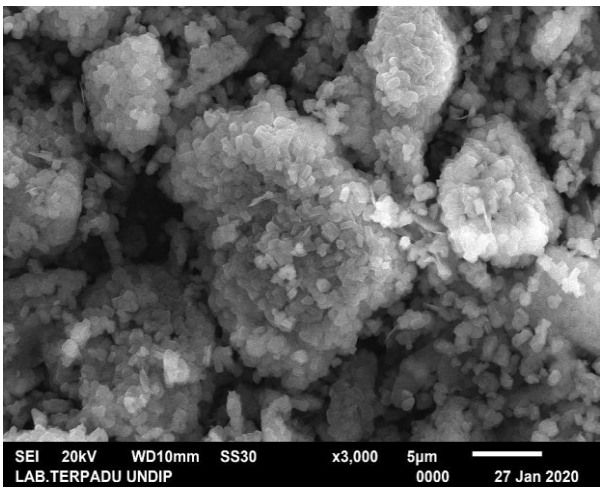

Figure 4. Surface morphology of HZSM-5

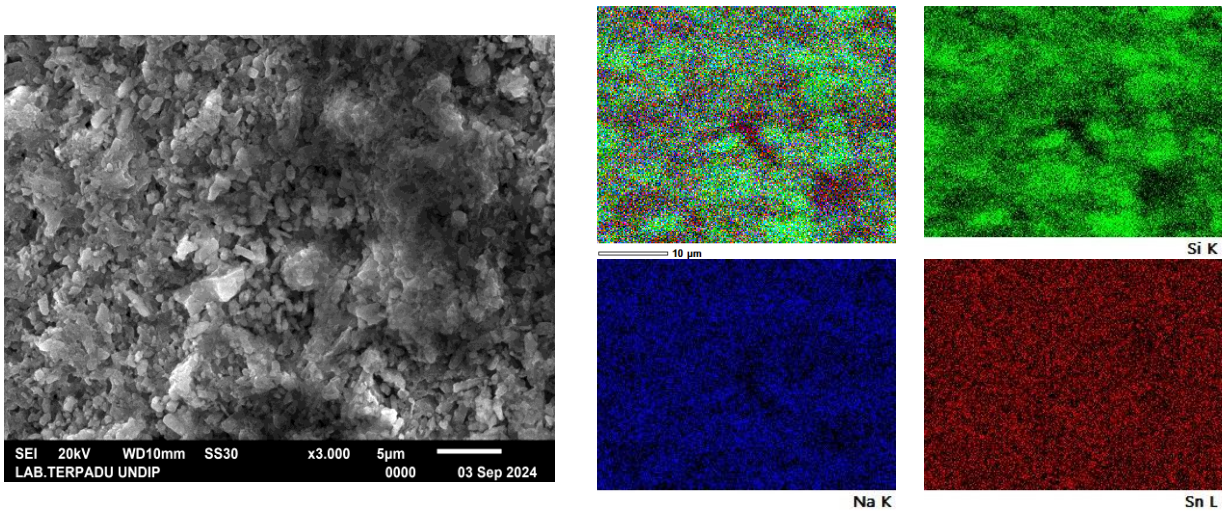

Figure 5. **Surface morphology and elemental mapping of $SnCl_2$/HZSM-5**

Table 2. **EDX result of HZSM-5 and $SnCl_2$/HZSM-5**

Compound	%mass	
	HZSM-5	$SnCl_2$/HZSM-5
SiO_2	56.89	57.74
Al_2O_3	29.3	21.27
C	12.8	18.36
Na_2O	-	0.06
SnO_2	-	1.98
Cl	-	0.59

The textural characteristics of HZSM-5 and $SnCl_2$/HZSM-5 were assessed for surface area, total pore volume, and average pore diameter. The results demonstrate that the impregnation of HZSM-5 with $SnCl_2$ modified its porosity and structural properties. The BET surface area of HZSM-5 is 293.696 m^2/g, whereas $SnCl_2$/HZSM-5 demonstrates a slightly smaller surface area of 292.510 m^2/g. This slight decrease indicates that the addition of $SnCl_2$ does not substantially modify the overall framework structure of the zeolite. The overall pore volume increases significantly from 0.163 cm^3/g (HZSM-5) to 0.261 cm^3/g ($SnCl_2$/HZSM-5), suggesting the incorporation of greater mesoporosity or modifications in pore interconnection resulting from the modification process. The average pore diameter significantly increases from 1.527 nm in HZSM-5 to 5.326 nm in $SnCl_2$/HZSM-5. The significant increase suggests that $SnCl_2$ impregnation leads to a structural rearrangement, possibly due to pore expansion effects. Adding Sn species could promote the formation of mesopores, hence improving molecular diffusion and catalytic efficacy, especially for bulky reactants in diverse catalytic applications (see Table 3).

Table 3. **Surface properties of HZSM-5 and $SnCl_2$/HZSM-5**

Properties	HZSM-5	$SnCl_2$/HZSM-5
Surface area (m^2/g)	293.696	292.510
Total pore volume (cm^3/g)	0.163	0.261
Average pore diameter (nm)	1.527	5.326

The enlargement of pore size observed by Castro et al. [36] in the production of Fe/ZnO/TiO_2 catalysts through impregnation is ascribed to the incorporation of Zn species, which interrupts the dense oxide structure and facilitates partial reconfiguration of the solid matrix. This structural reconfiguration generates additional voids and expands existing channels, thus establishing a more open, porous network that facilitates molecule transport during catalytic processes [36]. Increasing the pore diameter enhances reactant mobility throughout the porous network, hence improving esterification efficiency. Huang et al. (2021) discovered that the catalytic activity of hollow sulfonated mesoporous carbon spheres (HMCS-S) enhanced with increasing pore size, especially for long-chain fatty acids (C12). This

enhancement is associated with the optimal molecular diffusion capacity, which depends on the texture and surface characteristics of the HMCS-S. The findings demonstrated that larger pores enhance reactant accessibility, thereby increasing turnover frequency (TOF) in the catalytic process [37]. The structural modifications induced by $SnCl_2$ impregnation enhance both Lewis acidity and pore accessibility, thereby improving the effectiveness of the catalyst. The enlarged pore structure improves the mobility of larger reactants, such as castor oil and TMP, thereby reducing and improving the resistance. The synergistic enhancements facilitate more effective engagement with Sn^{2+} sites, leading to improved conversion and selectivity of polyol ester products [38].

$SnCl_2$/HZSM-5 was analyzed using X-ray diffraction (XRD) with a scanning range of 10° to 90°. The diffraction pattern reveals the crystalline structure of HZSM-5, as indicated by the distinctive peaks at 23.10°, 23.96°, and 24.0°, as denoted by the red circles in Figure 6. The peaks correspond to the MFI-type zeolite framework, suggesting that HZSM-5 retains its firmness after $SnCl_2$ impregnation [39]. Theoretically, SnO_2 ought to demonstrate diffraction peaks at 26.7°, 33.9°, and 54.8°; however, these peaks were not observed in the XRD results [40]. The absence of these peaks indicates that the Sn concentration in the impregnated HZSM-5 is relatively low, resulting in a dispersion of Sn species at either the atomic level or within a highly amorphous phase [41-43]. The XRD results suggest that the impregnation with $SnCl_2$ does not substantially modify the crystalline structure of HZSM-5 and introduces structural stability to the catalyst. The structural stability, along with the potential catalytic advantages of Sn loading, makes $SnCl_2$/HZSM-5 a promising material for ester oil production that requires both acidity and metal functionality [40].

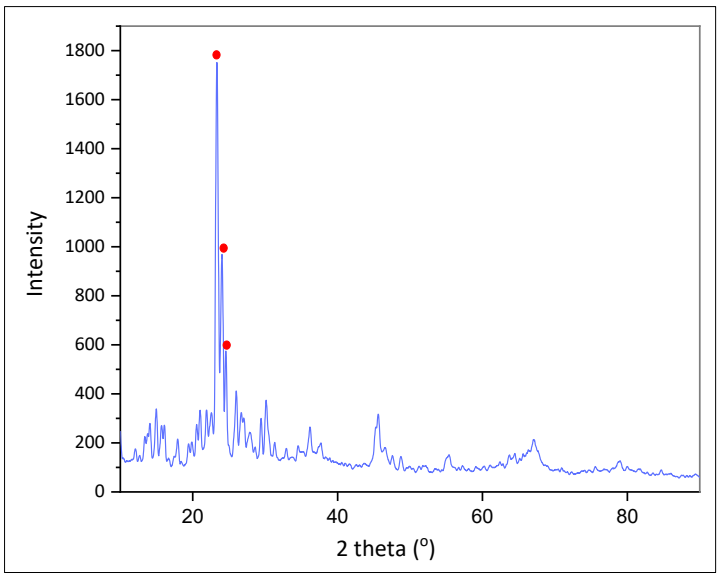

Figure 6. XRD result of $SnCl_2$/HZSM-5

3-2- Physicochemical Characteristics of The Ester Oil

Fourier Transform Infrared (FTIR) analysis was performed to identify the functional groups in the ester oil. Figure *7* illustrates the spectrum of the FTIR analysis result for the ester oil derived from castor oil and trimethylolpropane, subjected to esterification at a temperature of 130°C with a catalyst of $SnCl_2/H_2O$ 0.793% of the mass of castor oil. The X-axis of the graph denotes the wave number in cm^{-1}, and the Y-axis illustrates the percentage of transmittance. The transmittance percentage indicates the degree to which a substance allows infrared light to pass through at a specific wavenumber. The valleys on the graph represent the absorption of infrared radiation. The analysis result indicates the existence of valleys at wave numbers 3392.24 cm^{-1}, 2924.23 cm^{-1}, 2854 cm^{-1}, 1742.5 cm^{-1}, 1460 cm^{-1}, 1375.94 cm^{-1}, and 1162.82 cm^{-1}. The absorption at 3392.24 cm^{-1} exhibits the presence of hydroxyl groups (O-H), presumably derived by residual reactants or moisture in the sample [41]. The presence of methyl (C-H) and methylene (C-H) groups at 2924.23 cm^{-1} and 2854.3 cm^{-1} indicates the existence of aliphatic chains within the ester oil's structure. The strong absorption band at 1742.5 cm^{-1} corresponds to the stretching vibration of the carbonyl (C=O) group in the ester, a key indicator of the successful synthesis of the ester oil. The absorption at 1460 cm^{-1} and 1375.94 cm^{-1} indicates the presence of methyl or methylene groups, along with the symmetric bending vibration of CH_3, confirming the aliphatic structure in the ester oil [42]. The absorption band at 1162.82 cm^{-1} corresponds to the stretching vibration of C-O, a characteristic indicative of ester compounds [43]. The results reveal that the synthesized ester oil possesses a chemical structure consistent with ester properties. At the same time, residual signs of hydroxyl groups suggest the presence of water content in the oil. Water is a byproduct of the esterification reaction, as shown in Figure 2. The presence of water also indicates that the esterification reaction has occurred, but the evaporation process in a vacuum oven has not successfully removed the water.

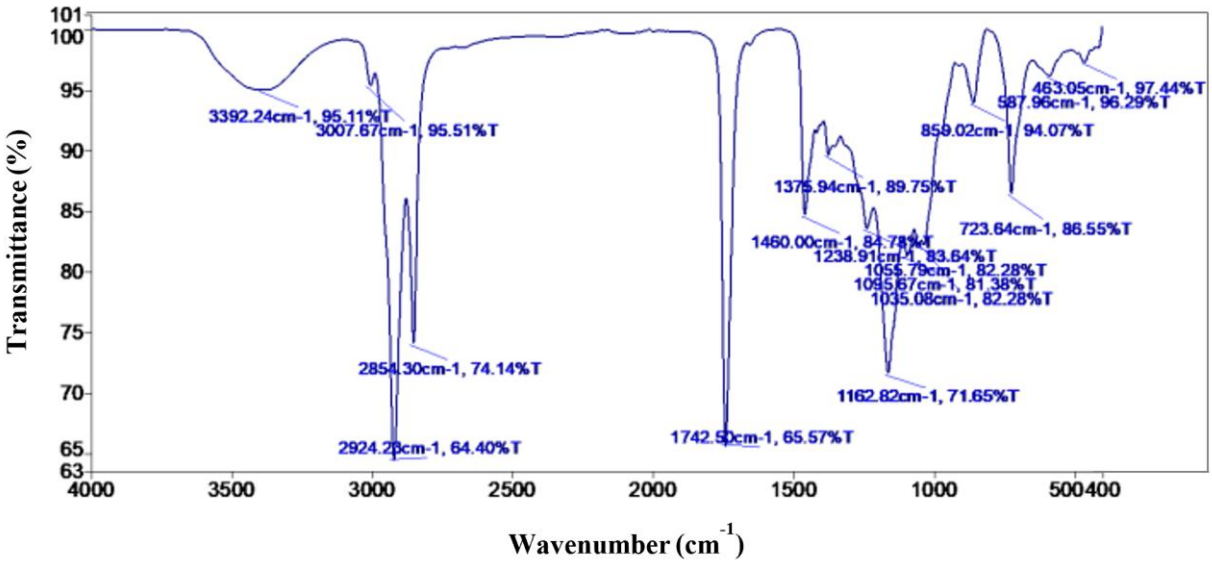

Figure 7. FTIR analysis of ester oil product

Table 4 shows the ester oil properties, with the samples' appearance, color, and PCB content meeting the standard parameters. The density at 20°C is an essential parameter in applying distribution transformer insulation. This parameter influences the efficacy of transformer insulating oil. The density of the synthesized ester oil ranges from 0.963 g/cm³ to 0.999 g/cm³. The number is within the standard limit, which is below 1 g/cm³. A lower density of transformer insulating oil correlates with increased dielectric strength and thermal conductivity, which are crucial for transformer efficiency [44].

The viscosity of ester oil affects its flow properties, influencing the oil's ability to dissipate heat and lubricate transformer components. Table 4 shows that the viscosity of the ester oil at 40°C ranges from 188.5 cSt to 251.8 cSt. The value exceeds the standard parameter of less than 50 cSt. Ester oils from natural sources often exhibit greater viscosity than mineral oils. Nonetheless, viscosity above the required standard parameter may impede the flow of insulating oil and potentially lead to overheating in transformers. The viscosity of the synthesized polyol ester oils is significantly higher compared to the standard range reported for insulating fluids sourced from non-edible feedstocks, including jatropha, karanja, neem, mahua, and rubber-seed oils (10–50 cSt at 40 °C), in addition to the synthetic esters commonly utilized in commercial applications (~29 cSt) [9]. The increased viscosity observed can be ascribed to the molecular properties of castor-oil-derived polyol esters, notably the existence of residual hydroxyl groups and the substantial three-branched configuration of the ricinoleic-based ester chains. These factors enhance intermolecular hydrogen bonding and limit flow mobility [45]. The hydroxyl group (-OH) exhibits polarity and can establish hydrogen bonds with other molecules in castor oil, including interactions with additional hydroxyl groups or carbonyl groups in esters. These hydrogen bonds enhance intermolecular attraction, making the fluid more movement-resistant and elevating its viscosity. This impacts the elevated viscosity of the resultant product [12, 14, 16].

The viscosity and acidity values of the synthesized ester oil slightly exceed the recommended standards in IEC 62975:2021; however, the consequences for practical insulating-fluid application are manageable and can be optimized through additional processes. To address these deviations, an additional strategy was implemented by employing a two-step transesterification route [46]. Joshi et al. [47] demonstrated that applying a two-step transesterification approach to waste cooking oil methyl ester using different alcohols effectively reduced the viscosity of the resulting ester oils to 24.9–44.9 cSt, values suitable for transformer insulating applications. Initially, castor oil was converted to a methyl ester using methanol and KOH. This was completed by a second esterification process involving trimethylolpropane (TMP) to modify the molecular structure further. $SnCl_2$ supported on Zeolite Y was utilized as the catalyst in the second esterification stage, yielding an ester oil with a significantly reduced viscosity of 16.50 cSt, within the IEC standard range and projected to improve flow behavior and cooling efficiency in transformer systems. Furthermore, improving conversion completeness and implementing post-treatment purification are expected to reduce acidity to acceptable levels, enabling the product to retain the intrinsic thermal and dielectric properties of polyol esters while meeting transformer-grade standards [48]. The acid value of the ester oil produced in this study ranges from 1.295 to 1.560 mg KOH/g oil, exceeding the standard of 0.08 mg KOH/g oil. Acidity is expressed as acid value, measured in mg KOH/g oil, which indicates the base required to neutralize the acid in the sample. The higher the acid value, the greater the sample's acidity. The acidity in ester oil may arise from free fatty acids (FFA) that have not completely reacted to produce products during the esterification process. Acidic substances exhibit polarity, indicating a disparity in charge distribution inside the molecule [49–51].

In addition to the standard insulating-oil requirements in IEC 62975:2021, conductivity testing was conducted to further assess the electrical suitability of the synthesised ester oil as a transformer-grade insulating fluid. The reaction product demonstrated non-conductive properties, suggesting a lack of detectable ionic species in the oil phase [52]. heterogeneous Sn-zeolite catalysts such as Sn-Beta have demonstrated the ability to preserve their overall Sn content after extensive use, with ICP-AES analysis revealing no significant decrease in Sn loading, thereby indicating minimal leaching into the liquid phase [53].

Table 4. Properties of ester insulation oil

Sample	Operating Temperature (°C)	Catalyst loading (%)	Appearance	Colour	Density at 20°C (g/cm³)	Viscosity at 40°C (cSt)	Acidity (mg KOH/g)
Ester insulator oil standard parameter (IEC 62975:2021)			Clear	<1.0	<1	<50	<0.6
Castor oil			Clear	<1.0	0.986	188.500	1.623
Sample A	130	0.793	Clear	<1.0	0.999	202.407	1.387
Sample B	130	1.5	Clear	<1.0	0.972	209.580	1.401
Sample C	130	2.207	Clear	<1.0	0.964	192.507	1.411
Sample D	120	2	Clear	<1.0	0.971	207.952	1.300
Sample E	120	1	Clear	<1.0	0.963	190.628	1.295
Sample F	115.858	1.5	Clear	<1.0	0.964	251.831	1.514
Sample G	140	2	Clear	<1.0	0.965	239.541	1.565
Sample H	144.142	1.5	Clear	<1.0	0.967	217.506	1.423
Sample I	130	1.5	Clear	<1.0	0.966	233.420	1.560
Sample J	140	1	Clear	<1.0	0.964	229.361	1.556

3-3- Statistics Analysis of Ester Oil Production Process Optimization

GCMS analysis identified methyl ester compounds in the sample, enabling the calculation of the yield value. Table 5 indicates that operational condition C (temperature 130°C, catalyst 2.207%) yields the highest ester oil production. In comparison to the work of Kamarudin et al. (2020), who reported only 35% conversion of waste cooking oil methyl ester with TMP after 4 hours, sample C's esterification obtained a high conversion of 93.09%, indicating greatly increased catalytic performance. This notable enhancement highlights the superior efficiency of the $SnCl_2$/HZSM-5 catalyst in activating hydroxyl-rich substrates and overcoming diffusion limitations typically observed in polyol ester synthesis [42]. As the response variable, the yield in the production of ester oil from castor oil and trimethylolpropane was examined by analysis of variance (ANOVA). This analysis aims to determine the significance of the variable's impact on yield as the response variable and to investigate the possibility of an optimal point within the range of the experimental variables. This experiment employs Linear, Quadratic, Special Cubic, and Cubic ANOVA models. The model determining significance in the ANOVA is selected to analyze the variables. ANOVA was performed using Design-Expert 13.0 software.

Model validation testing that accurately represents experimental data is performed by calculating the R^2 coefficient of determination. The R^2 coefficient ranges from 0 to 1. The analysis of variance (ANOVA) results demonstrate that the chosen model for yield response is quadratic, as it possesses the highest R^2 value compared to other models and is the one endorsed by DesignExpert. The R^2 score for the quadratic model is 0.9524 (Table 7). The model is selected based on the highest and nearest R^2 value. Significance tests for each model coefficient use the P-value, or probability value, which is usually related to the risk of incorrectly rejecting a hypothesis. The P-value can also be defined as a specific type of research error. The P-value determines the significance of the variable's influence on the resulting yield response. A variable is considered significant if its P value is less than the established significance level of 0.05. The ANOVA results in Table 6 show a P value of 0.0094, which is less than 0.05. This indicates a significant relationship between the independent variable and the response variable.

The lack-of-fit is the ratio of the lack-of-fit mean square and the pure error mean square. The F-value statistical test may determine the significance of the lack-of-fit error at the specified significance level (P-value) of 0.05. The lack-of-fit P-value in this study is 0.0378, indicating statistical significance. This signifies that while the model clarifies the majority of the association between the independent variable and the response variable, there remain patterns in the residual data that the model fails to account for. If the model and lack-of-fit are significant, it indicates that the model possesses predictive capability but is not yet ideal [54, 55]. The derived prediction model is yield = $46.03 - 0.7283\ A + 3.27\ B - 0.7798\ AB + 16.69\ A^2 + 0.0391\ B^2$, where A represents the catalyst loading and B denotes the operating temperature.

Table 5. Ester oil yield

Sampel	Operating temperature (°C)	Catalyst loading (%)	Ester oil yield (%)
A	130	0.793	78.114
B	130	1.5	64.687
C	130	2.207	81.770
D	120	2	57.084
E	120	1	54.803
F	115.858	1.5	45.268
G	140	2	63.224
H	144.142	1.5	52.856
I	130	1.5	45.836
J	140	1	64.061

Table 6. Analysis of variance from ester oil production optimization

Source	Sum of Squares	df	Mean Square	F-value	P-value	
Model	1648.01	5	329.60	16.02	0.0094	
A-Catalyst loading	4.24	1	4.24	0.2063	0.6733	
B-Operating temperature	85.34	1	85.34	4.15	0.1113	*significant*
AB	2.43	1	2.43	0.1182	0.7483	
A^2	1272.74	1	1272.74	61.87	0.0014	
B^2	0.0070	1	0.0070	0.0003	0.9862	
Residual	82.28	4	20.57			
Lack of Fit	82.21	3	27.40	377.76	0.0378	*significant*
Pure Error	0.0725	1	0.0725			
Cor Total	1730.29	9				

Table 7. ANOVA Regression

R^2	0.9524
Adjusted R^2	0.8930
Predicted R^2	0.6620
Adeq Precision	110.845

Figure 8 illustrates the contour and three-dimensional surface graphs of the optimization process for ester oil production. The red regions denote the highest response levels, whereas the blue areas represent the lowest response values. The points on the graph denote combinations of variables in the experiment. Variations in the independent variables (temperature and catalyst percentage) substantially influence the response. The color variations on the contour graph and the gradient of the 3D surface graph signify this. If the optimization seeks to maximize yield, the variable combinations in the red region are chosen. If the optimization has different objectives, then the variable combination selected resides in the blue area. The interaction between temperature and catalyst loading in ester oil production was also investigated. The results demonstrate that temperature is crucial in determining yield, with elevated temperatures (140°C) producing higher yields than lower temperatures (120°C). This trend indicates that increased temperatures accelerate reaction kinetics, facilitating more efficient esterification and transesterification processes [56].

An optimization study of methyl ester production from castor oil and methanol showed that the reaction rate increased to a specific point, producing a higher yield, then rapidly dropped when the temperature exceeded the methanol boiling point [57, 58]. The effect of catalyst concentration was investigated, demonstrating that yield improves with the addition of the catalyst. The increment of methyl ester yield during the increase in catalyst loading was observed in the methyl ester production from waste cooking oil and chicken fat oil using an acid catalyst. An increased catalyst loading will yield more active sites, thereby enhancing the conversion of free fatty acids (FFA) to fatty acid methyl esters (FAME) by reducing the activation energy, accelerating the reaction rate [59]. Higher viscosity with a higher catalyst loading is thought to cause the increase in methyl ester yield since it would reduce the diffusion between the three phases

of the system (alcohol, oil, and catalyst) [60, 61]. Further, the methyl ester yield decreased with the increase of catalyst loading. This may be correlated to the immiscibility of oil and alcohol, phase separation issues, and an increase in reaction mixture viscosity, which affects alcohol blending [61, 62]. Nonetheless, the trend shows a non-linear pattern, wherein more significant catalyst loading does not correspondingly increase the yield. This phenomenon is likely due to the saturation of active sites, resulting in reduced catalytic activity at elevated doses. The predicted optimal condition, with a yield of 64.509%, is obtained at a temperature of 140% and a catalyst concentration of 2%.

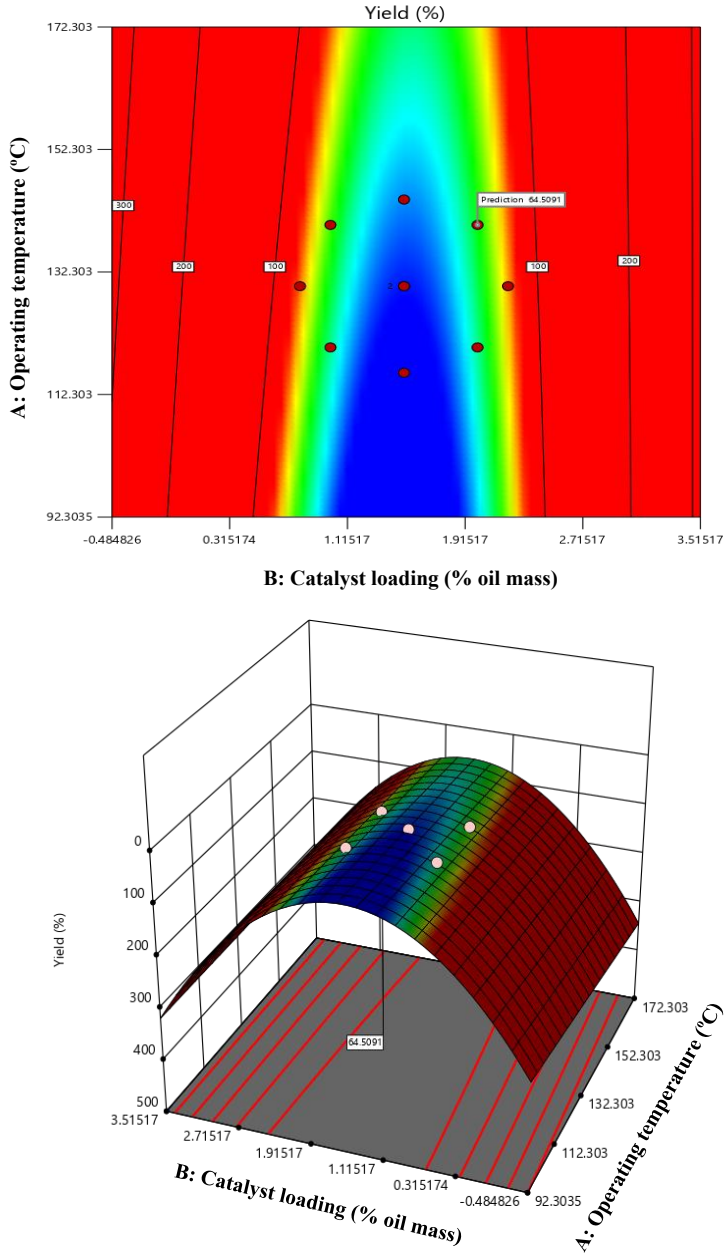

Figure 8. (a) Contour plot (b) 3D surface graph of optimization process

4- Conclusion

The esterification of castor oil with trimethylolpropane using $SnCl_2$/HZSM-5 as a heterogeneous catalyst yielded polyol ester oils with a maximum yield of 81.77% under optimized conditions of 130°C and 2.207 wt% catalyst loading. In fulfillment of IEC 62975:2021, the final product demonstrated a satisfactory appearance, density, and dielectric behavior appropriate for distribution-transformer insulating oil applications, and FTIR analysis verified the development of distinctive ester functional groups. The analysis using response surface methodology and ANOVA revealed that the established quadratic model is statistically significant ($R^2 = 0.952$), confirming that both temperature and catalyst dosage have a substantial impact on ester formation efficiency. Although the viscosity of the synthesised ester exceeds the recommended specifications, this property is related to the ricinoleic-based molecular structure of castor oil. Further improvements in conversion efficiency, tighter dehydration control, and post-reaction purification are anticipated to enhance flowability without compromising dielectric strength.

The catalytic properties of $SnCl_2$/HZSM-5, such as its pronounced Lewis acidity, hierarchical pore architecture that promotes the diffusion of larger reactants, and limited tin migration, highlight its potential for the sustainable production of polyol esters. To confirm the long-term safety and stability of the insulating oil, a more conclusive evaluation of metal leaching using inductively coupled plasma (ICP) analysis is advised in future studies, even though conductivity results and physicochemical behavior strongly suggest that Sn remains immobilized on the catalyst surface. Moving toward industrial implementation, future research will focus on long-term catalyst durability evaluation, continuous-flow operation, and improved heat- and mass-transfer performance for viscous feedstocks. Techno-economic and environmental evaluations will be necessary for evaluating the competitiveness of castor-derived ester oils as biodegradable, high-performance insulating fluids for power transformers.

5- Declarations

5-1- Author Contributions

Conceptualization, I. and W.W.; methodology, I., W.W., and J.P.; validation, S., K.G.H.M., and A.S.A.; formal analysis, I. and J.P.; investigation, J.P.; resources, I. and S.; data curation, H.; writing—original draft preparation, J.P.; writing—review and editing, W.W. and H.; visualization, J.P.; supervision, W.W., H., and S.; project administration, I.; funding acquisition, I. All authors have read and agreed to the published version of the manuscript.

5-2- Data Availability Statement

The data presented in this study are available on request from the corresponding author.

5-3- Funding

This research was supported by the Research Resource Collaboration Program of PT PLN (Persero) under Contract No. 0044.Pj/HKM.02.01/F30000000/2024.

5-4- Acknowledgments

The authors acknowledge PT. PLN (Persero) and Diponegoro University for providing institutional support and research facilities that made this work possible.

5-5- Institutional Review Board Statement

Not applicable.

5-6- Informed Consent Statement

Not applicable.

5-7- Conflicts of Interest

The authors declare that there is no conflict of interest regarding the publication of this manuscript. In addition, the ethical issues, including plagiarism, informed consent, misconduct, data fabrication and/or falsification, double publication and/or submission, and redundancies have been completely observed by the authors.

6- References

[1] Montano, L., Pironti, C., Pinto, G., Ricciardi, M., Buono, A., Brogna, C., Venier, M., Piscopo, M., Amoresano, A., & Motta, O. (2022). Polychlorinated Biphenyls (PCBs) in the Environment: Occupational and Exposure Events, Effects on Human Health and Fertility. Toxics, 10(7), 365. doi:10.3390/toxics10070365.

[2] Jacob, J., Preetha, P., & Krishnan, S. T. (2020). Review on natural ester and nanofluids as an environmental friendly alternative to transformer mineral oil. IET Nanodielectrics, 3(2), 33–43. doi:10.1049/iet-nde.2019.0038.

[3] Mukhopadhyaya, K., Aryan, A., & Rajeev, A. (2021). Analysis and Comparison of Characteristics of Biodegradable Transformer Oils. 2021 7th International Conference on Advanced Computing and Communication Systems, ICACCS 2021, 90–94. doi:10.1109/ICACCS51430.2021.9441728.

[4] Payus, C. M., Jikilim, C., & Sentian, J. (2020). Rainwater chemistry of acid precipitation occurrences due to long-range transboundary haze pollution and prolonged drought events during southwest monsoon season: climate change driven. Heliyon, 6(9), e04997. doi:10.1016/j.heliyon.2020.e04997.

[5] Siddique, A., Yaqoob, M., Aslam, W., Zaffar, F., Atiq, S., & Usama Shahid, M. (2024). A systematic review on promising development of cost-effective, biodegradable, and environment friendly vegetable-based nanofluids as a future resource for green transformer insulation oil. Journal of Molecular Liquids, 403(April), 124836. doi:10.1016/j.molliq.2024.124836.

[6] Oparanti, S. O., Rao, U. M., & Fofana, I. (2023). Natural Esters for Green Transformers: Challenges and Keys for Improved Serviceability. Energies, 16(1), 61. doi:10.3390/en16010061.

[7] Boris, H., Gockenbach, E., & Dolata, B. (2008). Ester fluids as alternative for mineral based transformer oil. 2008 IEEE International Conference on Dielectric Liquids, ICDL 2008, 4622541. doi:10.1109/ICDL.2008.4622541.

[8] Gockenbach, E., & Borsi, H. (2008). Natural and synthetic ester liquids as alternative to mineral oil for power transformers. Annual Report - Conference on Electrical Insulation and Dielectric Phenomena, CEIDP, 521–524. doi:10.1109/CEIDP.2008.4772928.

[9] Das, A. K., Chavan, A. S., Shill, D. C., & Chatterjee, S. (2021). Jatropha Curcas oil for distribution transformer – A comparative review. Sustainable Energy Technologies and Assessments, 46(April), 101259. doi:10.1016/j.seta.2021.101259.

[10] Lopresto, C. G. (2025). Sustainable biodiesel production from waste cooking oils for energetically independent small communities: an overview. International Journal of Environmental Science and Technology, 22(3), 1953–1974. doi:10.1007/s13762-024-05779-2.

[11] Wen, C., Shen, M., Liu, G., Liu, X., Liang, L., Li, Y., Zhang, J., & Xu, X. (2023). Edible vegetable oils from oil crops: Preparation, refining, authenticity identification and application. Process Biochemistry, 124(December 2022), 168–179. doi:10.1016/j.procbio.2022.11.017.

[12] Mubofu, E. B. (2016). Castor oil as a potential renewable resource for the production of functional materials. Sustainable Chemical Processes, 4(1), 1–12. doi:10.1186/s40508-016-0055-8.

[13] Mohan Rao, U., Fofana, I., Jaya, T., Rodriguez-Celis, E. M., Jalbert, J., & Picher, P. (2019). Alternative dielectric fluids for transformer insulation system: Progress, challenges, and future prospects. IEEE Access, 7, 184552–184571. doi:10.1109/ACCESS.2019.2960020.

[14] Patel, V. R., Dumancas, G. G., Viswanath, L. C. K., Maples, R., & Subong, B. J. J. (2016). Castor oil: Properties, uses, and optimization of processing parameters in commercial production. Lipid Insights, 9(1), 1–12. doi:10.4137/LPI.S40233.

[15] Dalvand, P., & Mahdavian, L. (2022). Biodiesel Production in the Presence of Eggshell Nano-Catalyst. Chemistry and Technology of Fuels and Oils, 58(1), 55–62. doi:10.1007/s10553-022-01351-1.

[16] Singh, S., Sharma, S., Sarma, S. J., & Brar, S. K. (2023). Roles of Process Parameters on the Ricinoleic Acid Production from Castor Oil by Aspergillus flavus BU22S. Fermentation, 9(4), 1–20. doi:10.3390/fermentation9040318.

[17] Casas, A., Ramos, M. J., Rodríguez, J. F., & Pérez, Á. (2013). Tin compounds as Lewis acid catalysts for esterification and transesterification of acid vegetable oils. Fuel Processing Technology, 106, 321–325. doi:10.1016/j.fuproc.2012.08.015.

[18] Kricheldorf, H. R., & Weidner, S. M. (2021). Polymerization of l-lactide with SnCl2: A Low Toxic and Eco-friendly Catalyst. Journal of Polymers and the Environment, 29(8), 2504–2516. doi:10.1007/s10924-020-02042-w.

[19] Su, H., Zhao, Q., Jiang, C., Wang, Y., Niu, Y., Li, X., Lou, W., Qi, Y., & Wang, X. (2023). Preparation of highly dispersed SnO/TiO2 catalysts and their performances in catalyzing polyol ester. RSC Advances, 13(13), 8934–8941. doi:10.1039/d2ra07334j.

[20] Potchamyou Ngatcha, A. D., Zhao, A., Zhang, S., Xiong, W., Sarker, M., Xu, J., & Alam, M. A. (2023). Determination of active sites on the synthesis of novel Lewis acidic deep eutectic solvent catalysts and kinetic studies in microalgal biodiesel production. RSC Advances, 13(15), 10110–10122. doi:10.1039/d3ra00543g.

[21] Schwiderski, M., & Kruse, A. (2015). Catalytic effect of aluminium chloride on the example of the conversion of sugar model compounds. Journal of Molecular Catalysis A: Chemical, 402, 64–70. doi:10.1016/j.molcata.2015.03.018.

[22] Heeley, K., Orozco, R. L., Sheppard, I., Macaskie, L. E., Love, J., & Al-Duri, B. (2025). Assessment of Iron(III) chloride as a catalyst for the production of hydrogen from the supercritical water gasification of microalgae. Next Energy, 6(September 2024), 100198. doi:10.1016/j.nxener.2024.100198.

[23] Sun, H., Yang, J., Sun, M., Wei, Z., Xu, X., Zhang, Y., Dai, J., Zhang, J., & Shao, Z. (2025). Lewis Acid-Mediated Interface Engineering for Enhanced Electrocatalytic Energy Conversion. Advanced Functional Materials, 19393, 1–22. doi:10.1002/adfm.202519393.

[24] Sarker, M. I., Ngo, H., Sharma, B. K., Wagner, K. M., Jones, K. C., & Powell, M. J. (2023). Green synthesis of trimethylolpropane triisostearate and triisooleate for usage as bio-lubricants. Tribology International, 186(April), 108649. doi:10.1016/j.triboint.2023.108649.

[25] Da Silva, M. L., Figueiredo, A. P., Cardoso, A. L., Natalino, R., & Da Silva, M. J. (2011). Effect of water on the ethanolysis of waste cooking soybean oil using a tin(II) chloride catalyst. JAOCS, Journal of the American Oil Chemists' Society, 88(9), 1431–1437. doi:10.1007/s11746-011-1794-z.

[26] Lemaire, P., de Reviere, A., Sharma, D., Ruaux, V., Al Atrach, J., Valtchev, V., Thybaut, J., Sabbe, M., & Verberckmoes, A. (2025). The Influence of Mesopore Architecture in Hierarchical H-ZSM-5 on n-Butanol Dehydration. ACS Engineering Au, 5(4), 434–449. doi:10.1021/acsengineeringau.5c00033.

[27] Karaman, B. P. (2024). Nickel and cobalt incorporated mesoporous HZSM-5 catalysts for biofuel production from bio-oil model compounds. Research on Chemical Intermediates, 50(9), 4465–4483. doi:10.1007/s11164-024-05357-8.

[28] Mi, M., Xiong, J., Zhang, S., Zhang, Y., Chen, X., Shao, R., Xu, W., & Ding, J. (2024). Catalytic Esterification of Pentaerythritol over a Mesoporous Composite SnCl2@HZSM-5 Catalyst. ChemistrySelect, 9(22), 1–8. doi:10.1002/slct.202401172.

[29] Mostafa Marzouk, N., Abo El Naga, A. O., Younis, S. A., Shaban, S. A., El Torgoman, A. M., & El Kady, F. Y. (2021). Process optimization of biodiesel production via esterification of oleic acid using sulfonated hierarchical mesoporous ZSM-5 as an efficient heterogeneous catalyst. Journal of Environmental Chemical Engineering, 9(2), 105035. doi:10.1016/j.jece.2021.105035.

[30] Zhao, B., Yang, P., Zhang, N., Inns, D. R., Kozhevnikova, E. F., Katsoulidis, A. P., Kozhevnikov, I. V., Steiner, A., & Zhang, H. (2024). Sulfonated hierarchical ZSM-5 zeolite monoliths as solid acid catalyst for esterification of oleic acid. Chemical Communications, 60(91), 13356–13359. doi:10.1039/d4cc05044d.

[31] Riswanto, F. D. O., Rohman, A., Pramono, S., & Martono, S. (2019). Application of response surface methodology as mathematical and statistical tools in natural product research. Journal of Applied Pharmaceutical Science, 9(10), 125–133. doi:10.7324/JAPS.2019.91018.

[32] Singh, W. R., & Singh, H. N. (2024). CCD-RSM optimization of biodiesel production from waste cooking oil using Angulyagra oxytropis and Bellamya crassa snail shell-based heterogeneous catalysts. Fuel, 378(August), 132953. doi:10.1016/j.fuel.2024.132953.

[33] Mohamad Dzol, M. A. A., Balasundram, V., Shameli, K., Ibrahim, N., Manan, Z. A., & Isha, R. (2022). Catalytic pyrolysis of high-density polyethylene over nickel-waste chicken eggshell/HZSM-5. Journal of Environmental Management, 324(September), 116392. doi:10.1016/j.jenvman.2022.116392.

[34] Tian, H., He, H., Jiao, J., Zha, F., Guo, X., Tang, X., & Chang, Y. (2022). Tandem catalysts composed of different morphology HZSM-5 and metal oxides for CO_2 hydrogenation to aromatics. Fuel, 314, 123119. doi:10.1016/j.fuel.2021.123119.

[35] Mohammed, I. Y., Abakr, Y. A., & Kazi, F. K. (2018). In-situ Upgrading of Napier Grass Pyrolysis Vapour Over Microporous and Hierarchical Mesoporous Zeolites. Waste and Biomass Valorization, 9(8), 1415–1428. doi:10.1007/s12649-017-9925-x.

[36] Castro, L., Matheus, L., Lenzi, G., Arantes, M., Almeida, L., Brackmann, R., & Colpini, L. (2025). Assessment of the Effect of Zn Co-Doping on Fe/TiO2 Supports in the Preparation of Catalysts by Wet Impregnation for Photodegradation Reactions of Food Coloring Effluents. Colorants, 4(2), 17. doi:10.3390/colorants4020017.

[37] Huang, L., Song, C., Liu, Y., Lin, H., Ye, W., Huang, H., Lu, R., & Zhang, S. (2021). Enhancement of catalytic esterification by tuning molecular diffusion in sulfonated carbon. Microporous and Mesoporous Materials, 318(January), 111024. doi:10.1016/j.micromeso.2021.111024.

[38] Xie, W., Wang, H., & Li, H. (2012). Silica-supported tin oxides as heterogeneous acid catalysts for transesterification of soybean oil with methanol. Industrial and Engineering Chemistry Research, 51(1), 225–231. doi:10.1021/ie202262t.

[39] Zhang, Y., Zhou, Y., Huang, L., Xue, M., & Zhang, S. (2011). Sn-modified ZSM-5 As support for platinum catalyst in propane dehydrogenation. Industrial and Engineering Chemistry Research, 50(13), 7896–7902. doi:10.1021/ie1024694.

[40] Philia, J., Widayat, W., Sulardjaka, S., Nugroho, G. A., & Darydzaki, A. N. (2023). Aluminum-based activation of natural zeolite for glycerol steam reforming. Results in Engineering, 19(April), 101247. doi:10.1016/j.rineng.2023.101247.

[41] Philia, J., Widayat, W., & Sulardjaka, S. (2022). Amorphous adsorbent from geothermal solid waste for methylene blue removal. Journal of Environmental Engineering and Science, 18(1), 1–9. doi:10.1680/jenes.21.00082.

[42] Kamarudin, N. S. B., Veny, H., Sidek, N. F. B., Abnisa, F., Sazali, R. A., & Aziz, N. (2020). Investigation on synthesis of trimethylolpropane (TMP) ester from non-edible oil. Bulletin of Chemical Reaction Engineering and Catalysis, 15(3), 808–817. doi:10.9767/BCREC.15.3.8862.808-817.

[43] Kaye, S., Shriner, R. L., & Fuson, R. C. (1948). The Systematic Identification of Organic Compounds. Journal of Criminal Law and Criminology (1931-1951), 39(1), 132. doi:10.2307/1138600.

[44] Abdi, S., Harid, N., Safiddine, L., Boubakeur, A., & Haddad, A. (2021). The correlation of transformer oil electrical properties with water content using a regression approach. Energies, 14(8), 1–14. doi:10.3390/en14082089.

[45] Pathmasiri, T. K. K. S., Perera, G. I. P., & Gallage, R. (2022). Investigation of palm-castor oil blends as base stocks of bio-lubricants for industrial applications. Energy Sources, Part A: Recovery, Utilization and Environmental Effects, 44(1), 1354–1374. doi:10.1080/15567036.2019.1643425.

[46] Nogales-Delgado, S., Encinar, J. M., & González, J. F. (2023). A Review on Biolubricants Based on Vegetable Oils through Transesterification and the Role of Catalysts: Current Status and Future Trends. Catalysts, 13(9), 1299. doi:10.3390/catal13091299.

[47] Joshi, J. R., Bhanderi, K. K., Patel, J. V., & Karve, M. (2023). Chemical modification of waste cooking oil for the biolubricant production through transesterification process. In Journal of the Indian Chemical Society, 100(3), 100909. doi:10.1016/j.jics.2023.100909.

[48] Raof, N. A., Hamid, H. A., Mohamad Aziz, N. A., & Yunus, R. (2022). Prospects of Plant-Based Trimethylolpropane Esters in the Biolubricant Formulation for Various Applications: A Review. Frontiers in Mechanical Engineering, 8(February), 1–21. doi:10.3389/fmech.2022.833438.

[49] Roslan, N. A., Zainal Abidin, S., Abdullah, N., Osazuwa, O. U., Abdul Rasid, R., & Yunus, N. M. (2022). Esterification reaction of free fatty acid in used cooking oil using sulfonated hypercrosslinked exchange resin as catalyst. Chemical Engineering Research and Design, 180, 414–424. doi:10.1016/j.cherd.2021.10.020.

[50] Satriadi, H., Pratiwi, I. Y., Khuriyah, M., Widayat, Hadiyanto, & Prameswari, J. (2022). Geothermal solid waste derived Ni/Zeolite catalyst for waste cooking oil processing. Chemosphere, 286(P1), 131618. doi:10.1016/j.chemosphere.2021.131618.

[51] Prameswari, J., Widayat, W., Buchori, L., & Hadiyanto, H. (2023). Novel iron sand-derived α-Fe2O3/CaO2 bifunctional catalyst for waste cooking oil-based biodiesel production. Environmental Science and Pollution Research, 30(44), 98832–98847. doi:10.1007/s11356-022-21942-z.

[52] Hussain, M., Mir, F. A., & Ansari, M. A. (2022). Nanofluid transformer oil for cooling and insulating applications: A brief review. Applied Surface Science Advances, 8, 100223. doi:10.1016/j.apsadv.2022.100223.

[53] Peeters, E., Khalil, I., Eloy, P., Calderon-Ardila, S., Dijkmans, J., Ferrini, P., Debecker, D. P., Taylor, R. A., Douvalis, A. P., Dusselier, M., & Sels, B. F. (2021). Tandem Reduction-Reoxidation Augments the Catalytic Activity of Sn-Beta Zeolites by Redispersion and Respeciation of SnO2Clusters. Chemistry of Materials, 33(23), 9366–9381. doi:10.1021/acs.chemmater.1c03265.

[54] Olatunji, O. M., Horsfall, I. T., & Ubom, E. V. (2021). Response surface optimization approach to predict the maximum %biodiesel yield via transesterification of esterified shea butter oil by utilizing bio-catalysts. Current Research in Green and Sustainable Chemistry, 4(August), 100167. doi:10.1016/j.crgsc.2021.100167.

[55] Passerine, B. F. G., & Breitkreitz, M. C. (2024). Important Aspects of the Design of Experiments and Data Treatment in the Analytical Quality by Design Framework for Chromatographic Method Development. Molecules, 29(24), 6057. doi:10.3390/molecules29246057.

[56] Huda, M. S., Odegaard, M., Chandra Sarker, N., Webster, D. C., & Monono, E. (2024). Enhancing Recovery Yield of Vegetable Oil Methyl Ester for Bioresin Production: A Comparison Study Using Acid Neutralization. ChemEngineering, 8(1), 16. doi:10.3390/chemengineering8010016.

[57] Ismail, S., Ahmed, A. S., Anr, R., & Hamdan, S. (2016). Biodiesel Production from Castor Oil by Using Calcium Oxide Derived from Mud Clam Shell. Journal of Renewable Energy, 2016, 1–8. doi:10.1155/2016/5274917.

[58] Angassa, K., Tesfay, E., Weldmichael, T. G., & Kebede, S. (2023). Response Surface Methodology Process Optimization of Biodiesel Production from Castor Seed Oil. Journal of Chemistry, 2023. doi:10.1155/2023/6657732.

[59] Shatesh Kumar, Shamsuddin, M. R., Farabi, M. S. A., Saiman, M. I., Zainal, Z., & Taufiq-Yap, Y. H. (2020). Production of methyl esters from waste cooking oil and chicken fat oil via simultaneous esterification and transesterification using acid catalyst. Energy Conversion and Management, 226(August), 113366. doi:10.1016/j.enconman.2020.113366.

[60] Ali, R. M., Elkatory, M. R., & Hamad, H. A. (2020). Highly active and stable magnetically recyclable CuFe2O4 as a heterogenous catalyst for efficient conversion of waste frying oil to biodiesel. Fuel, 268(January), 117297. doi:10.1016/j.fuel.2020.117297.

[61] Sandouqa, A., Al-Hamamre, Z., & Asfar, J. (2019). Preparation and performance investigation of a lignin-based solid acid catalyst manufactured from olive cake for biodiesel production. Renewable Energy, 132, 667–682. doi:10.1016/j.renene.2018.08.029.

[62] Bhatia, S. K., Gurav, R., Choi, T. R., Kim, H. J., Yang, S. Y., Song, H. S., Park, J. Y., Park, Y. L., Han, Y. H., Choi, Y. K., Kim, S. H., Yoon, J. J., & Yang, Y. H. (2020). Conversion of waste cooking oil into biodiesel using heterogenous catalyst derived from cork biochar. Bioresource Technology, 302(January), 122872. doi:10.1016/j.biortech.2020.122872.